Detection of wood species and defects with NIR

Thomas Grahn, Zakiya Yassin

RISE Report : 2023:24

Content

Summary 3
1 Introduction 4
2 Characterization method 5
3 Samples, measurements 6
4 Model calculation 7
5 Conclusions 20
6 References 22

Summary

In this project the possibility to determine different wood species and detect defects on wood cross-sections on logs with hyperspectral near-infrared camera was investigated. This project was a laboratory study where cross-sections of logs were scanned at the wood and fibre analysis laboratory at RISE with near-infrared instrument.

Wood samples from different origins and species, with different defects were scanned with a hyperspectral near-infrared camera. Classification models were developed to characterise and classify the different logs.

Spruce and pine samples were collected from different sawmills, a group of these samples contained fungal growth. The defects within the collected logs varied and some samples contained decay fungi such as sap- and heart rot as well as non-destructive blue stain.

Classifications models to distinguish between different wood species were developed, as well classification models to differentiate between healthy wood and the fungal attack were also developed.

1 Introduction

In the sawmill the wood raw material has strong influences on end product properties. To improve quality on products it is important to better classify and characterize logs in sawmills. Examples of important classification properties are wood species and defects such as different types of wood decay. The defects caused by decay are often difficult to detect visually. This classification is today done manually/visually where an operator visually selects defected logs. There is a risk that a large number of defect logs can be mislabelled as defect-free, thus sawmills need well functional and effective detection methods.

RISE has unique instruments to analyse, characterise and compare different wood materials. The hyperspectral imaging near-infrared (NIR) spectroscopy system gives the opportunity for characterisation of wood materials regarding physical and chemical properties. Previous studies have shown that NIR is a good tool to quantify different chemical properties as well as physical properties.

In this project the investigation to use hyperspectral imaging NIR to detect wood decay and classify the wood logs into different wood species was tested. Models and tools were developed for the prediction of different types of wood decay. Spruce and pine samples, with different degrees of wood decay, were collected from sawmills to be scanned and analysed in this test.

1.1.1 Wood characterisation using 2D NIR

The scanner

The hyperspectral imaging NIR instrument is composed of the following layout: A camera detector (320x256 pixels) was connected to a spectrograph that works in a way that it only will be a line in the centre of the camera’s 2D field of view that was measured at each measurement. The spectrograph was connected in its turn to a changeable lens that resulted in different field of views. Within the spectrograph the reflected NIR light from the 320 pixels was divided into NIR spectra, resulting in 320 NIR spectra with 256 wavelengths for each reading of the camera detector. The samples were illuminated with two ramps with halogen lamps, and the diffuse reflectance was collected and recorded by the camera. A conveyor moved the samples in front of the camera while scanning.

Depending on the various applications the NIR camera could be adapted to scan at different resolutions since the scanner has an exchangeable lens option. A micro-lens, for example, gives the opportunity to scan samples at a high spatial resolution (30 µm) but with a narrow field of view.

In this project, a wider field of view was needed, so the lens with a lower spatial resolution capability (1,0 mm) was used. This setting is more relevant to a future possible on-line application.

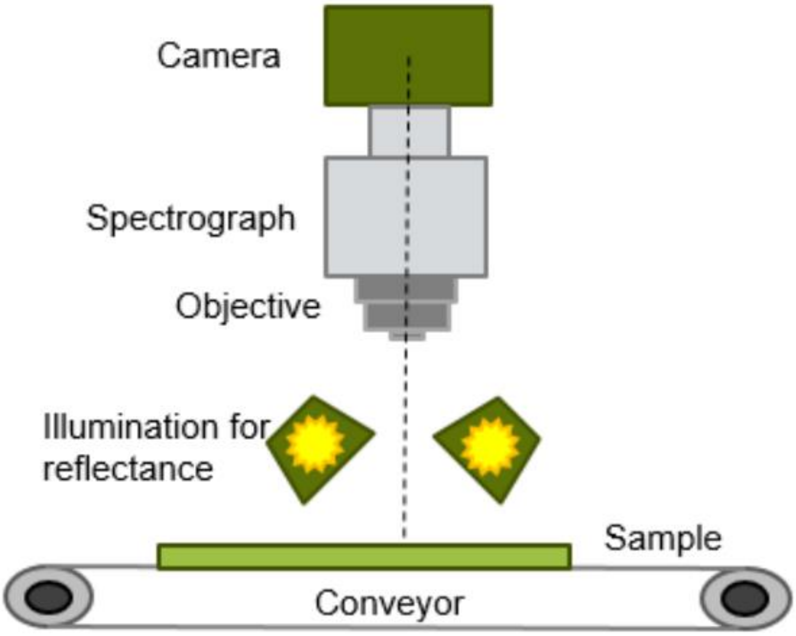

Figure 1. Principle sketch over the layout of a 2D NIR scanner

2 Characterization method

An efficient technique to characterize material properties (chemical and physical) is near infrared spectroscopy. Within the forest industry NIR has been used for physical and chemical characterisation in various applications, such as determination of moisture content, wood density as well as different chemical properties such as lignin and extractive content. (Scheepers *et al.*, 2019).

Since NIR-modelling and prediction is an indirect method, calibration data is needed to be able to associate the collected spectra to the different classes/properties included in the study. To achieve good models, it is necessary that the reference samples are correctly classified/analysed. The quality of prediction models is strongly affected by the analyses of the reference samples. Thus, accurate classification of wood species as well as fungal growth is important.

Calibration dataset

The calibration dataset for the classification models was built based on visual assessment. Pixels from different areas within the surfaces of the cross-sectional logs were selected and then assigned to the different classes.

The data set for the first classification model, wood species, included pixels from defect as well as healthy wood, and from different locations such as sapwood and heartwood within the surface area. The spectra from these selected pixels were assigned to the spruce and pine classes.

The same procedure was followed for building the dataset for the sap- and heartwood model. Pixels from sap- and heartwood surface areas were selected from both wood species and from defect and healthy logs.

Based on visual assessment the areas representing the different defects were selected, the spectra representing healthy wood areas were selected from completely healthy logs.

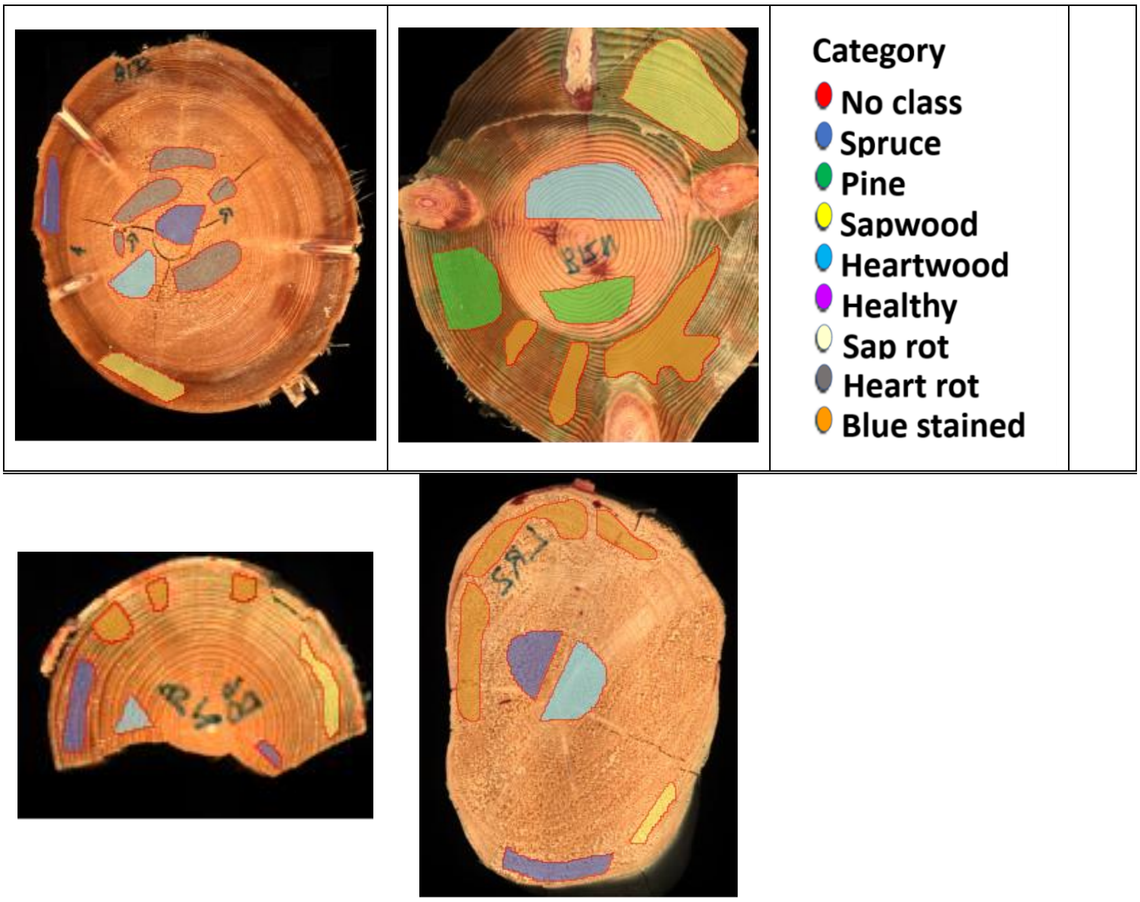

Figure 2: Visualization how the different pixels representing different classes where selected.

The software Breeze was used to form the dataset, to select the surfaces representing the different classes to form the different datasets and then to develop the different models.

3 Samples, measurements

A total of 125 samples were collected from the sawmills. Logs were from two different species, spruce and pine, and with different defects. In Table 1 the number of samples per species and sawmill is summarized.

Table 1: The different wood species for the logs collected from the different sites.

Origin	Number of samples	Pine	Spruces
Setra- Hasselfors	59	0	59
SCA- Munksund	54	54	0
Setra-NYBY	12	11	1

Table 2 shows the number and type of defects from each sawmill.

Table 2: The different defects within the logs collected from the different sites.

Origin	Healthy	Heart rot	Sap rot	Blue strain
Setra-Hasselfors	17	20	17	5 (surface blue stained)
SCA- Munksund	15	14	4	21
Setra-NYBY	0	0	0	12

It was difficult to obtain certain types of rot while collecting the samples at the sawmills. In both Hasselfors and Munksund the collected sap-rot samples may be somewhat untypical. It was difficult to get sap-rot at the times when the sampling was done and in the collected samples the decay may have progressed to long which have an effect on how the surface of the log looks. These samples were old and had been at the woodyard for a long time and may not be fully representable. As for blue stained samples, a good number of blue stained samples was collected in Nyby and Munksund but unfortunately no typical blue stained sample were collected from Hasselfors (spruce). The few samples found in Hasselfors were only samples with surface blue stained.

Collected samples were marked at site, with the help from personnel from Biometria. The different defects were marked with a black marker for each sample. Each sample was stored individually in a plastic bag.

All samples were stored in freezer to preserve the moisture content until scanning. Before scanning, samples were placed in a well-conditioned laboratory environment with temperature equal to 23 degrees Celsius and 43 % relative humidity.

4 Model calculation

Two types of models were built during this study. PCA-models (Principal component analysis) were used to understand if the NIR spectra can separate between the different classes of wood, species and defects. PLS-DA model (Partial least squares discriminant analysis) was used to classify the different wood species and differentiate between the healthy and defect wood surfaces.

Principle component analysis (PCA) is a statistical method used to better understand the relationship between different variables. It describes the composition of variances and covariances through several linear combinations of the primary variables. This technique allows a better visualisation of the variation within the dataset. In this study PCA-models were also built for segmentation. That is these models were used to exclude the background and extract the relevant data (spectra) from the scanned log.

Partial least squares discriminant analysis (PLS-DA) is an adaption of partial least square regression (PLS) technique which is used to find relations between two matrices: the X matrix (in this case the spectral data from NIR scanning) and the Y matrix (the different properties/ classes). When Y is categorical the technique used is PLS-DA. In this project PLS-DA models were developed to differentiate between the different classes. The PLS-DA models were developed to differentiate between these properties:

- Wood species: pine and spruce
- Type of wood: sapwood and heartwood.
- Healthy and the different defects within the logs: healthy, sap-rot, heart-rot and blue stain.

Hierarchical models

The different models were connected in a hierarchical workflow, to be able to predict the right property relying on previous information.

The workflow of the hierarchical flow is shown in Figure 3 below.

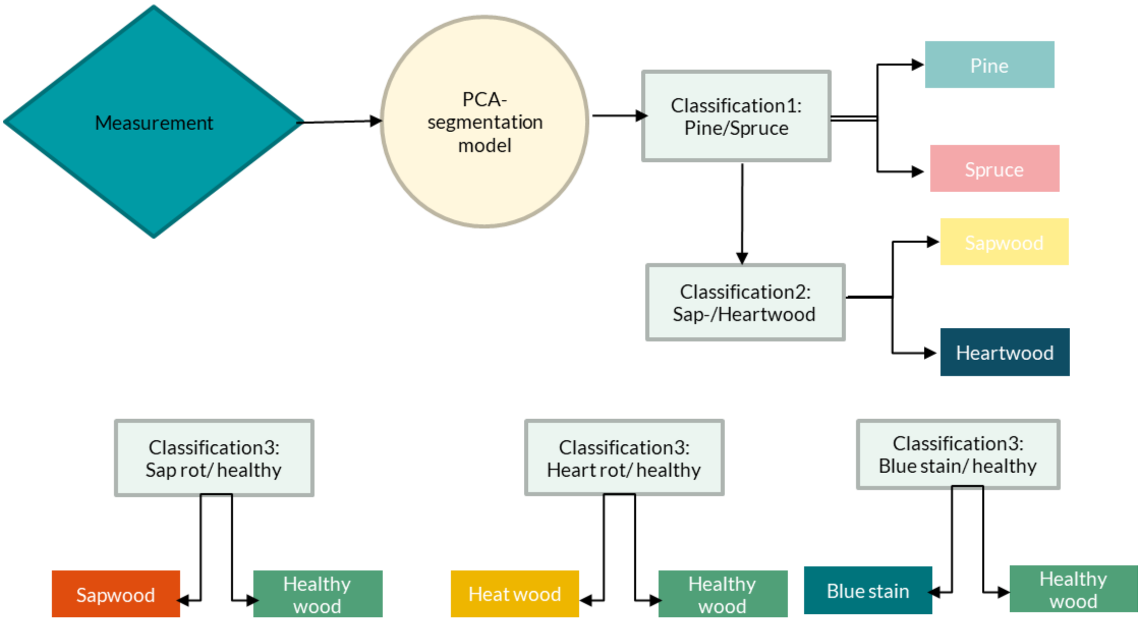

Figure 3: Diagram showing the workflow for the hierarchical models.

Blue stain and sap rot defects are mostly localized in the sapwood wood area, a model that takes into consideration and classifies the sapwood may better predict whether the logs have sap rot or blue stain decay. Heart rot on the other hand as its name suggests is mostly present in the heartwood area of the logs.

Sapwood and heartwood are chemically distinct for spruce and pine and different models for different species can be useful to help better predict the wood type.

To form the calibration dataset for the respective models, pixels from different areas (surfaces) were selected manually. Spectra representing healthy samples were selected from complete healthy samples to avoid assigning spectra to a wrong class due to contamination. Spectra representing the different defects were selected from homogenous surfaces.

Data from the average spectra representing these areas were used to build PLS-DA models as well as data from representative spectra from these areas (10 random pixels/area and their representative spectra) were compiled to build the different PLS-DA models.

PLS-DA models:

Classification model for pine versus spruce

To differentiate between the different wood species, a PLS-DA model was built to classify the different wood logs. Samples included were pine and spruce. Different areas were selected from healthy and defect wood as well as areas including sap- and heartwood. For each selected area average spectra were extracted and included in the dataset to reduce noise.

A different approach to build the data set was to include 10 random and unique representative spectra from the pixels within the chosen areas.

Table 3: The statistical parameters for the pine vs spruce PLS-DA models (manual and representative spectra)

PLS-da Pine vs Spruce		Number of samples	Training set	Test set	R^2	Q^2	$RMSEP$
	Average spectra	52	38	14	0,82	0,51	0,25
	Representative spectra	52	38	14	0,54	0,43	0,37

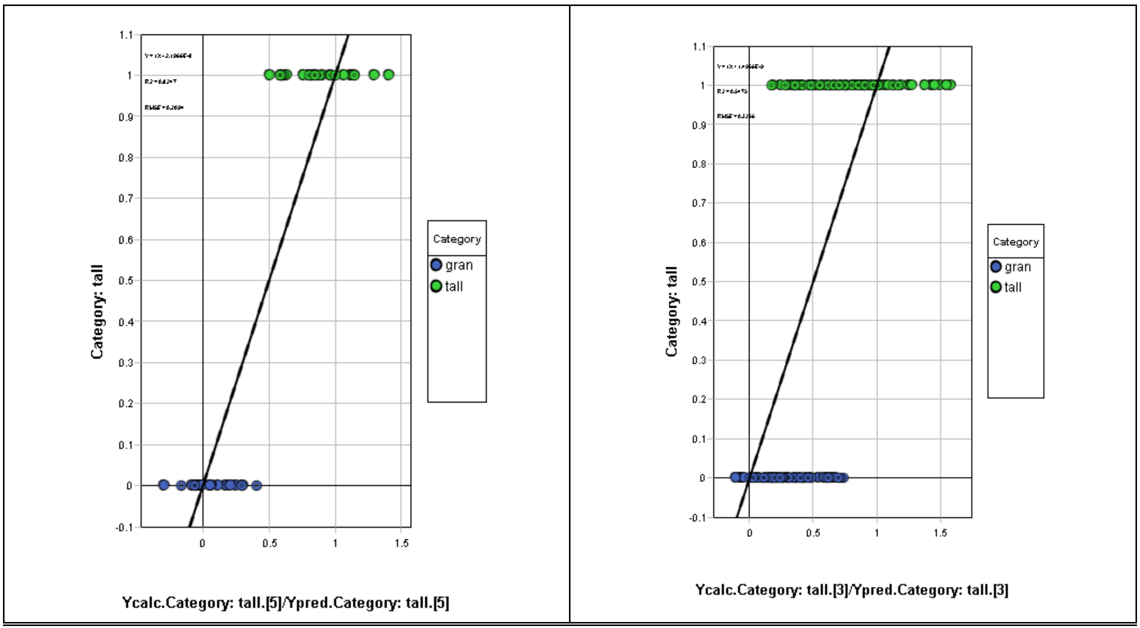

(a) (b)

Figure 4: The predicted (x-axis) vs the observed (y-axis) pine and spruce wood species for the average spectra pixels (a) and representative spectra (b) from manual selected areas.

As shown in the Table 3, the classification model from the first approach (average spectra from the selected areas) is better than that for the second approach. R^2 or the "goodness to fit" shows how good the model describes the variation within the X-variable. R^2 varies between 0 and 1, a higher value shows a better performance of the built model. Q^2 "goodness to predict" shows how well the models can predict new samples. Q^2 varies also between 0 and 1. $RMSEP$ "the root mean square error of prediction", the lower RMSEP the better ability for the models to predict new samples with less uncertainty. The RMSEP is based on the distance between the categories, which is equal to 1 in this case.

Comparing the two approaches show that the PLS-DA for wood species is better for the average spectra approach, as this model has a higher R^2, Q^2 and lower $RMSEP$.

When plotting the predicted versus the observed classes as show is Figure 4 a good separation between the two classes is obtained with the model from the average spectra, whereas representative spectra gave less separation between the two classes.

Classification model for sap- versus heartwood

Three different PLS-DA models were built to classify sap- and heartwood. Classification models for each wood species (spruce and pine) and a classification model from data from both species were used together. These models were based on the average spectra from the chosen surfaces representing the two different classes.

Table 4 shows the statistical parameters of the different models. The model for pine was much better than that for spruce. A classification model based on data from both species was acceptable, as both R^2 and Q^2 are acceptable.

Table 4: The statistical parameters for the sap vs heartwood PLS-DA models (for pine, spruce and both species)

	Average spectra	Number of samples	Training set	Test set	R^2	Q^2	$RMSEP$
PLS-da Sap- vs heartwood	Both wood species	55	42	13	0,78	0,61	0,30
	Pine	54	43	11	0,81	0,71	0,38
	Spruce	36	32	4	0,54	0,39	0,13

In Figure 5 the predicted versus the observed plots for the classification of sapwood and heartwood are shown. A good separation between sap and heartwood is obtained for pine as well as the model for both wood species. As for the PLS-DA model for spruce, a slight overlap occurred in the categorization of sapwood and heartwood.

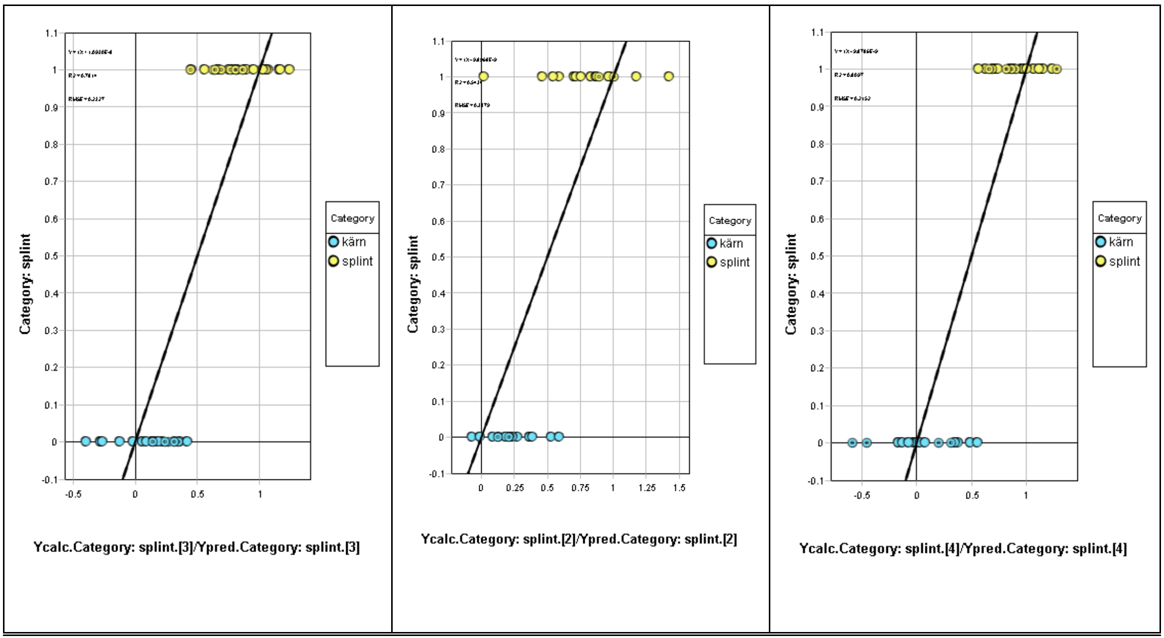

(a) Both pine and spruce

(b) Spruce

(c) Pine

Figure 5: The predicted (x-axis) versus the observed (y-axis) sap- and heartwood areas for the average spectra pixels from manually selected areas for both pine and spruce wood species (5a) for only spruce (5b) for pine (5c)

Classification model for sap rot versus healthy surfaces

The statistical parameters for the two different approaches (average and representative spectra) for the PLS-DA model (sap rot versus healthy surfaces) are represented in Table 5. Both models were strong and show good ability to predict new samples, as both R^2 and Q^2 are high.

Table 5: The statistical parameters for the saprot and healthy surfaces PLS-DA models (manual and represntative spectra)

PLS-da Sap rot and healthy surfaces		Number of samples	Training set	Test set	R^2	Q^2	$RMSEP$
	Average spectra	24	16	8	0,82	0,75	0,28
	Representative spectra	24	16	8	0,91	0,85	0,28

In Figure 6 the observed versus the predicted classes plot are shown for both approaches for separation of wood with sap rot from healthy wood is showed. In this case the model was developed for both pine and spruce together. The model was good and the fact that the models were built on both species was good. It indicated that the model could detect the rot itself and was not dependent on the extra information of the species. A slight overlap between the two classes was obtained for the model for the representative spectra.

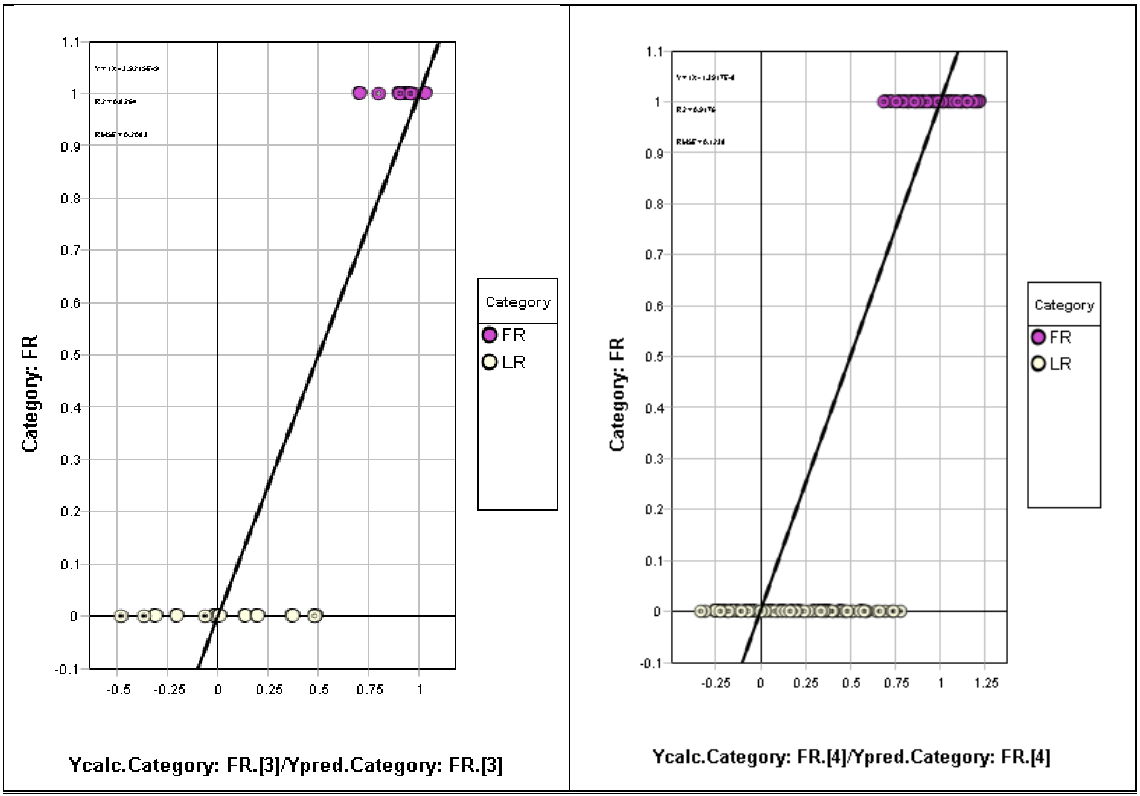

(a) (b)

Figure 6: The predicted (x-axis) vs the observed (y-axis) sapwood rot vs healthy wood areas for the average spectra pixels (a) and for the representative spectra (b) from manually selected areas for both pine and spruce wood species.

Classification model for heart rot versus healthy surfaces

Two classification models were built to classify heart rot and healthy wood were developed. The statistical parameters for the two approaches, the average spectra as well as the representative spectra for the manually chosen areas are shown in Table 6. The first model is better as it has a higher R^2 and lower $RMSEP$ error.Table 6: The statistical parameters for the heartrot and healthy surfaces PLS-DA models (manual and represntative spectra)

PLS-da Heart rot and healthy surfaces		Number of samples	Training set	Test set	R^2	Q^2	$RMSEP$
	Average spectra	62	46	16	0,81	0,54	0,30
	Representative spectra	62	46	16	0,70	0,60	0,56

In Figure 7 the plots for observed versus predicted classes for both approaches is shown for the models for separation of heart rot from healthy wood are shown. In this case the model was developed for both pine and spruce together. The model was good and the fact that the models were built on both species is good. It indicates that the model could detect the rot itself and was not dependent on the extra information of the species. An overlap between the two classes was observed for the model built from the representative spectra.

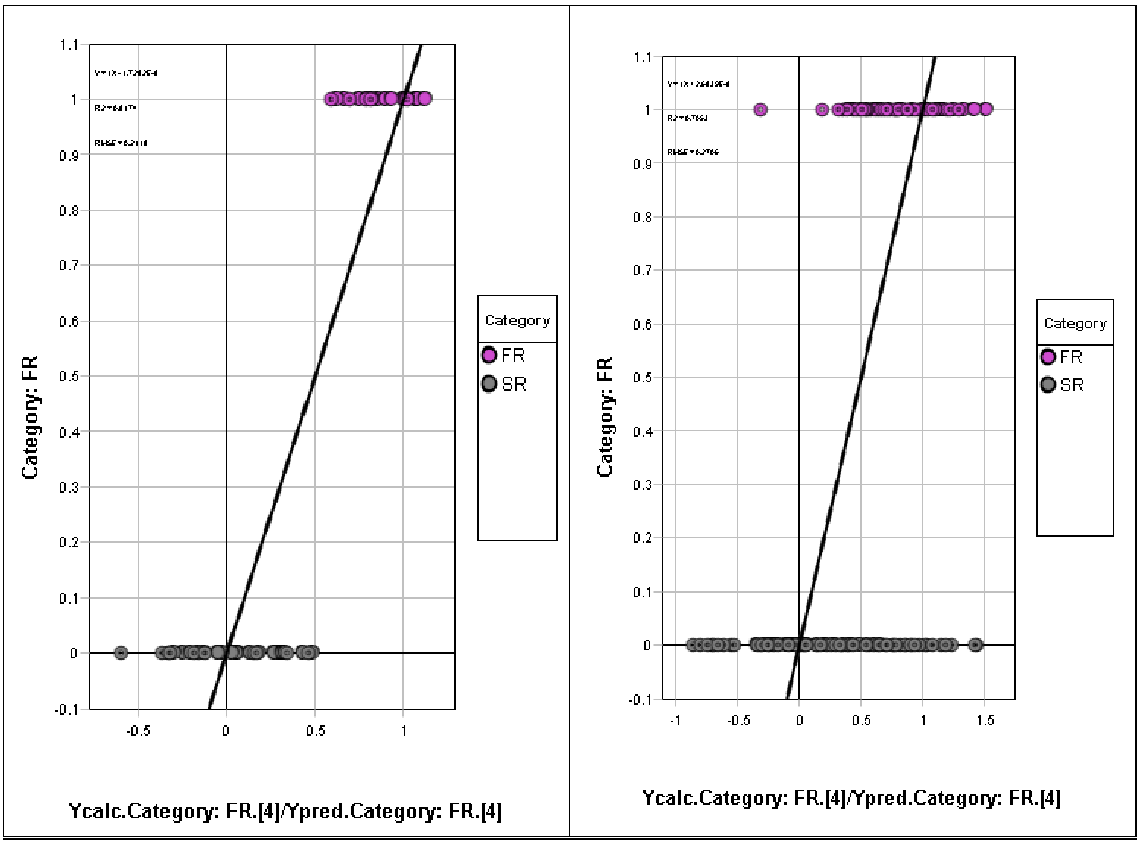

(a) (b)

Figure 7: The predicted (x-axis) vs the observed (y-axis) heartwood rot vs healthy wood areas for the average spectra pixels (a) and for the representative spectra (b) from manually selected areas for both pine and spruce wood species.

Classification model for blue stain versus healthy surfaces

As for the other two defects (heart rot and sap rot), the same process was followed to build models for the blue stain and healthy surfaces. The data included was from both wood species (spruce and pine). As shown in Table 7 the same results were obtained for blue stain models, a better model with higher R^2 and Q^2 was obtained for the average spectra model.

Table 7: The statistical parameters for the blue stain and healthy surfaces PLS-DA models (manual and represntative spectra)

PLS-da Blue stain and healthy surfaces		Number of samples	Training set	Test set	R^2	Q^2	$RMSEP$
	Average spectra	48	36	12	0,84	0,78	0,20
	Representative spectra	48	36	12	0,79	0,67	0,32

Figure 8 shows the observed versus predicted classes for the two different approaches. A good separation between blue stain and healthy wood classes was obtained for the average spectra model. An overlap between the two classes was obtained for the second approach.

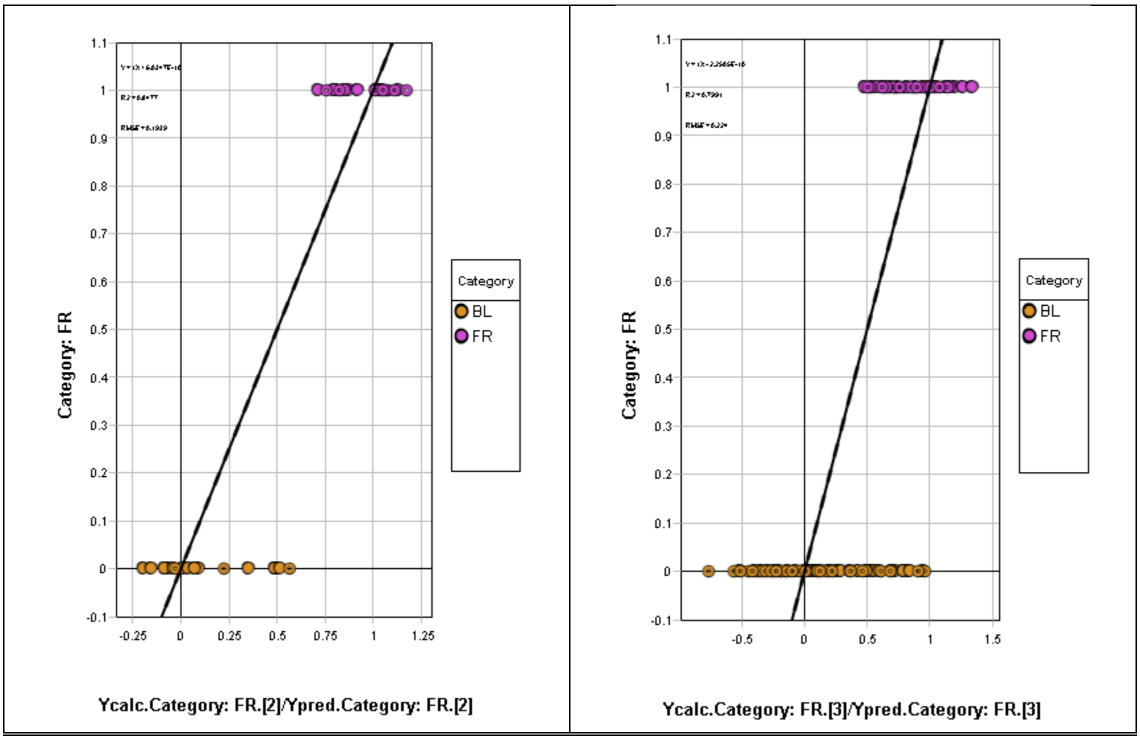

(a) (b)

Figure 8: The predicted (x-axis) vs the observed (y-axis) blue stain wood vs healthy wood areas for the average spectra pixels (a) and for the representative spectra (b) from manually selected areas for both spruce wood species.

All developed models clearly indicated that it was possible to separate species and defects in wood. However, all models were developed from the average of regions. This means that the noise in the images was reduced. To fully understand the potential of the methods the models need to be applied on another set samples not included in the modeling. This is a different scenario since the areas for the respective wood classes would not be known. The models themselves should identify these areas. In this case the spectra would not be possible to improve by reducing the noise for the defective areas.

Prediction

To get a better understanding on how good the models were, some samples (not included in the calibration dataset) were classified with the various PLS-DA models.

Two different approaches were used to test the different models. A prediction of every pixel within the cross-sectional scanned area, as well as a grid-sectional prediction *i.e.,* the cross-sectional areas were divided into grids, the majority of the properties predicted and assigned to this area were then annotated as the property of the specific area. The second approach was to make the prediction less sensitive to noise, *i.e.,* to make the data in the predictions more like the averages for the different regions used in the modeling. Figure 9 is a visualization of the workflow for the two different approached used to predict the samples.

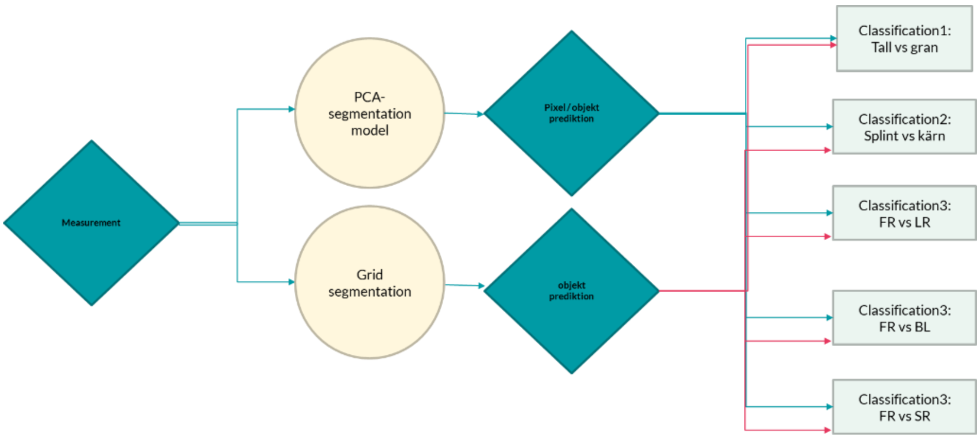

Figure 9: Diagram showing the Prediction workflow.

For example, Figure 10 shows predictions on one spruce cross-section. At the top there is an ordinary image, the other six images are predictions done with the models, the three in the middle row are pixel based and the three in the bottom row are grid-based prediction. The grid size was 9x9 pixels corresponding to 9x9 mm^2.

In the images to the left wood species classification was attempted. The pixel-based predictions illustrate the problem with noise in the image, some of the pixels were predicted as pine. When the predictions were grid-based the model for the species classified the log correctly as a spruce log.

In the images in the middle column sapwood and heartwood was classified. The sapwood-heartwood model predictions were more complicated to evaluate. The pixel-based predictions indicated a sapwood region for the whole circumference, but with rather few sapwood classified pixels in the "south-eastern" region. When the grid method was used instead some areas in the “northern” part and the “eastern” region were miss-labelled. The classification was based on the most frequent pixel in the grid, alternative ways to do this could be tested. Also, the size of the grid could be altered.

In the images to the right, heart rot and healthy wood were classified. The heart rot- healthy wood model prediction was good with both the pixel and grid-based prediction methods. The area containing heart rot was predicted correctly. Combining this model with a good sap-heartwood model would enhance the results and thus exclude possible errors if no heart rot was found in sapwood area. This is however based on visual assessment. A more definitive analysis is needed to evaluate whether the visual assessment was right or not.

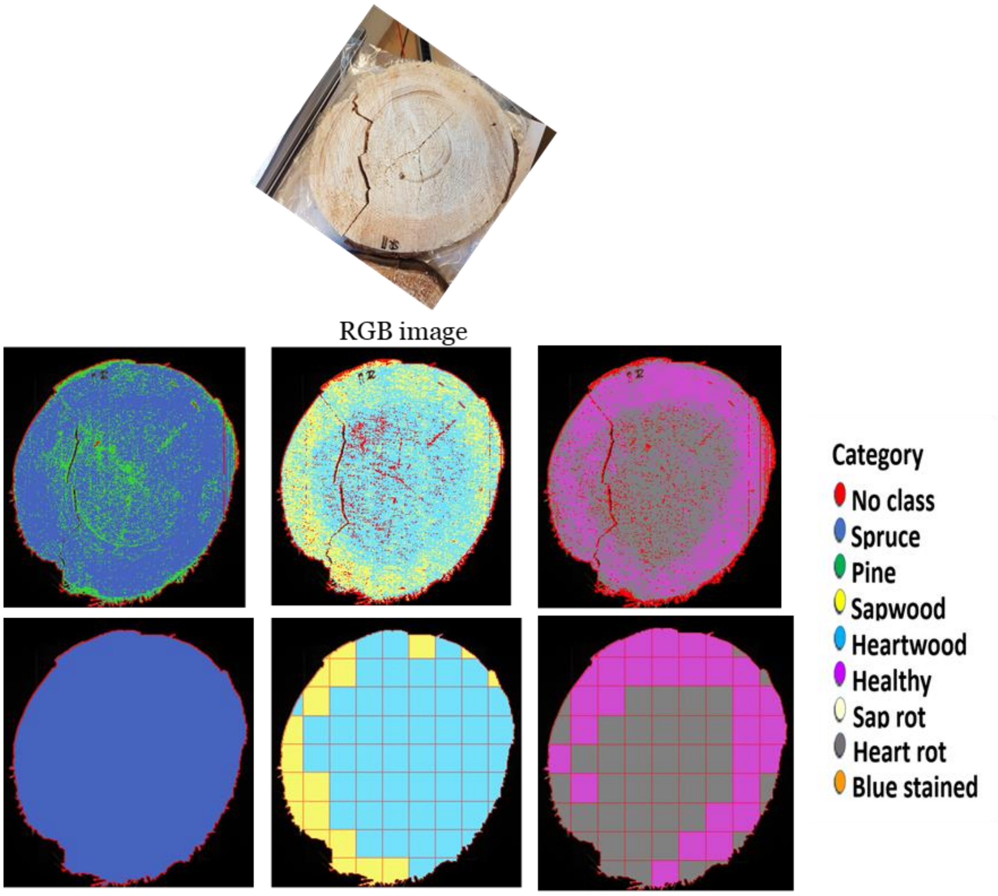

Figure 10: Illustration of the different approaches predicting the spruce heartwood rot log.

Figure 11 shows another example of predictions but in this case on one pine cross-section. The same layout as for the previous example is followed *i.e.*, at the top there is an ordinary image, the other six images are predictions done with the models, the three in the middle row are pixel based and the three in the bottom row are grid-based predictions. The grid size was 9x9 pixels corresponding to 9x9 mm^2. The pixel-based predictions illustrate the problem with noise in the image, some of the pixels were predicted as spruce. When the predictions were grid-based the model for the species classified the log correctly as pine in the image to the bottom left.

In the second column of images, the sapwood-heartwood model predictions were more complicated to evaluate. Even though some pixels around the sapwood area were predicted as sapwood, but this was not enough to be able to predict correctly at the grid- level.

As for the blue stain-healthy wood model, the model was able to correctly predict the blue stained surfaces as defects in the images to the right.

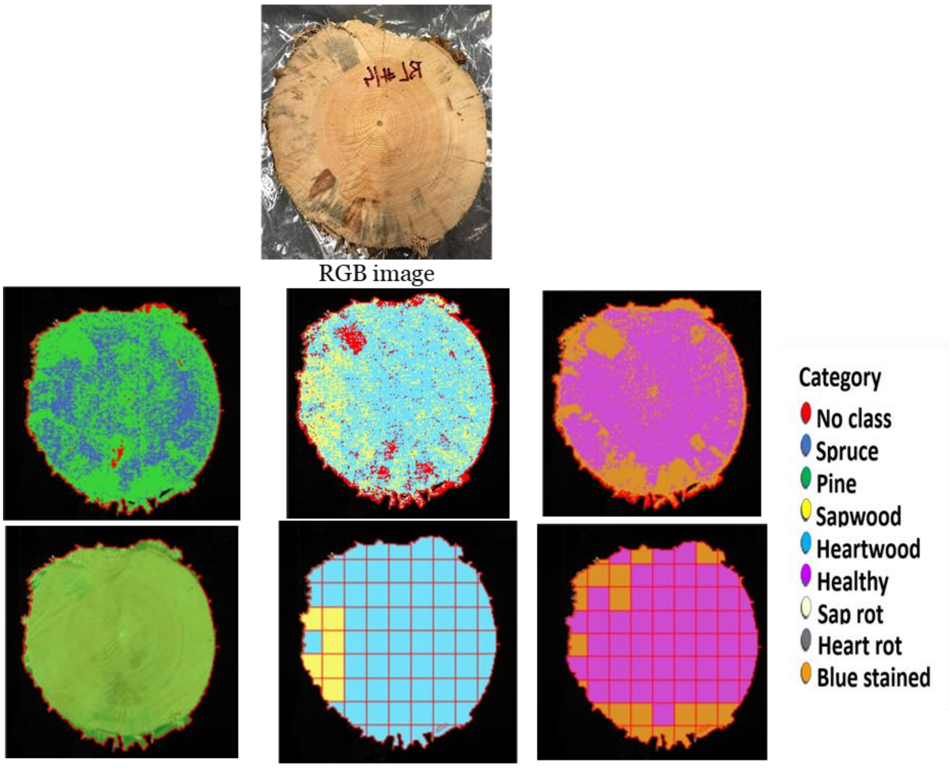

Figure 11: Illustration for the different approaches predicting the blue stained pine log.

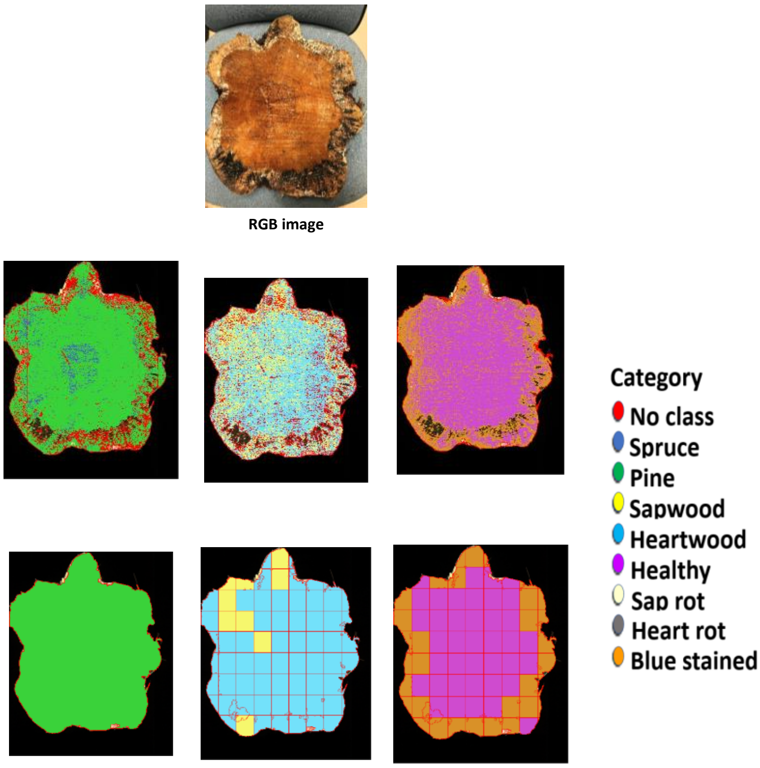

Figure 12: Illustration for the different approaches predicting the blue stained pine log (the natural surface)

Figure 12 shows another example of predictions but in this case the prediction was done on the natural surface of one pine cross-section. The same layout as for the previous examples is followed *i.e.*, at the top there is an ordinary image, the other six images are predictions done with the models, the three in the middle row are pixel based and the three in the bottom row are grid-based predictions. The grid size was 9x9 pixels corresponding to 9x9 mm². The pixel-based predictions illustrate the problem with noise in the image, some of the pixels were predicted as spruce. When the predictions were grid-based the model for the species classified the log correctly as pine in the image to the bottom left.

In the second column of images, the sapwood-heartwood model predictions were more complicated to evaluate. Even though some pixels around the sapwood area were predicted as sapwood, but this was not enough to be able to predict correctly at the grid- level.

As for the blue stain-healthy wood model, the model was able to correctly predict the blue stained surfaces as defects in the images to the right.

It is important to note that a high number of pixels was not classified, this is due to the fact that the models were built from pixels from clean-cut surfaces, enhancing the models and including data from the more natural surfaces.

To get a better understanding on how good the classification models are, the models were applied to samples that were not included in the calibration dataset. The results from the prediction of the various models from both the clean-cut surface logs as well as the natural surfaces are shown in the figures below.

Figure 13 shows the confusion matrix for the average spectra PLS-DA model for pine and spruce classes. The results shown are based on the majority of the pixels predicted of the surface of the sample scanned, from a total of 112 samples: 87,5% of the samples were predicted right, while 12,5% samples of the samples were classified wrong.

Spruce vs pine PLS-DA model

True class

Predicted class	98 (87,5%)	14 (12,5%)

Figure 13: Confusion matrix for the PLS-DA wood species model for the clean-cut surfaces.

The same was done for the other three defect models, the different models were applied to the same number of samples (112). Figure 14 shows the percentage of the right and wrong classified samples. These results are based on the majority of the predicted pixels per pixel, compared with a visual observation of the selected samples. About 3% of the healthy wood samples were predicted as defective samples and according to the models these samples contained sap rot. A further examination of this sample is needed to accurately define if this sample is defective or not. The sap rot and blue stain samples were categorized correctly. Some difficulties were encountered with the heart rot models. About 7% of the samples containing heart rot (based on visual assessment) were classified as healthy logs. To be able to make a better assessment a definitive analysis is needed for these samples as well.

Healthy vs defect PLS-DA models

True class

Predicted class		Healthy wood	Sap rot	Blue stain	Heart rot
	Healty wood	31, (96,87%)			7, (20,6%)
	Sap rot	1, (3,13%)	22, (100%)		
	Blue stain		0	24, (100%)	
	Heart rot			0	27, (79,4%)

Figure 14: Confusion matrix for the PLS-DA defect vs healthy wood models for the clean-cut surfaces.

The same analysis was applied to dirty crosscut surfaces that are encountered at sawmills. The goal was to get an understanding on how good these models are while scanning in a real-world environment.

These models were applied on 17 samples with natural/dirty surfaces. The results for Pine-spruce PLS-DA model are shown in Figure 15. The model had the ability to predict 76,4% of these samples correctly.

Spruce vs pine PLS-DA model

True class

Predicted class	13 (76,4%)	4 (23,6%)

Figure 15: Confusion matrix for the PLS-DA wood species model for the dirty surfaces.

The results for the different defect models, including sap- and heart rot as well as blue stain classification models are shown in Figure 16. As expected more wrong classification for the different defect models was obtained when classifying dirty surfaces. One of the healthy wood samples was classified as defective (included sap rot). As mentioned previously a different analysis is needed to see if this prediction was correct or not. Even though the sap rot model succeeded in predicting all the samples right, the blue stain and heart rot models had a higher number of wrong predictions.

Healthy vs defect PLS-DA models

True class

Predicted class		Healthy wood	Sap rot	Blue stain	Heart rot
	Healty wood	4, (80%)		2, (50%)	1, (25%)
	Sap rot	1, (20%)	5, (100%)		
	Blue stain		0	2, (50%)	
	Heart rot			0	3, (75%)

Figure 16: Confusion matrix for the PLS-DA defect vs healthy wood models for the natural surfaces.

5 Conclusions

In general, one can conclude that the first PLS-DA model (spruce vs pine) has a high ability to predict the samples with low error. The model however is based on the average spectra of the selected pixels and suffers from noise at the pixel levels.

Sapwood versus heartwood model for spruce was not as good as that for pine. This was expected since the level of extractives within the heartwood for spruce is less than that for pine and since many of the samples were old and dry it was not either possible to classify the wood based on moisture content. The classification model for both wood species is acceptable. However, when these models were applied to test samples and predicted on pixel level, it was difficult to differentiate between sap- and heartwood areas since a lot of noise at the pixel level were obtained. When applying the object grid prediction method, the models also failed to predict clear sap and heart areas. Currently the classification is based on the most frequent pixel in the grid, alternative ways to for this could be tested. Also, the size of the grid may be altered.

It was difficult to collect typical samples containing sap rot, the samples collected were old and dry and have been lying in the sawmill yard for a long time at the time of collection. The PLS-DA model to classify sap rot from healthy wood was good and was able to predict new samples with low error level. More typical samples are needed to do the right assessment.

Samples containing blue stain wood included in the dataset to build the models were from one wood species (pine) as no typical blue stain samples from spruce wood species were collected. Only few blue stain samples were found, and these samples were only surface blue stain. The PLS-DA models were good and were able to predict with low error levels.

A good number of heart rot samples were collected from both spruce and pine wood species. The classification model built to classify heart rot from healthy wood was strong. However, higher level of error was obtained when applying the classification model on new samples.

The analysis was based on the majority of the predicted class per grid, and an alternative for better results can be smaller grid prediction areas and alternative percentage of the predicted class per grid *i.e.*, if for example more than 30% of pixels are predicted as a certain defect the grid is defect.

To be able to draw a conclusion on how good these samples are an alternative reference method is needed to be able to draw a clear and accurate separation line between the healthy and defected areas. The assessment was based on visual analysis of the scanned samples, a better approach would be to study defected areas with microscopy on the fiber level to decide which areas are defective or not. This was, however, not possible to include in this project.

As for the ability of these models to classify dirty surfaces, it was difficult to draw a conlusion on the accuracy of the models. Applying the models on a larger number of logs containing dirty surfaces would help draw clearer conclusions on how well can these models perform when predicting non-clean surfaces logs. Another approach would be to expand the calibration dataset, including data from dirty surfaces in the models.

Different complementary techniques such and image analysis combined with NIR can help to improve the models further. Cameras combining the visual and NIR region is also an interesting technique to test.

6 References

Scheepers G., Z. Yassin, T. Grahn, T. Niittylä, E. Mellerowicz and H. Tuominen. 2019. High resolution phenotyping of greenhouse samples with SilviScan and NIR-imaging. The 34th Biennial IUFRO Tree Biotechnology Meeting. June 2019.

Through our international collaboration programmes with academia, industry, and the public sector, we ensure the competitiveness of the Swedish business community on an international level and contribute to a sustainable society. Our 2,800 employees support and promote all manner of innovative processes, and our roughly 100 testbeds and demonstration facilities are instrumental in developing the future-proofing of products, technologies, and services. RISE Research Institutes of Sweden is fully owned by the Swedish state.

I internationell samverkan med akademi, näringsliv och offentlig sektor bidrar vi till ett konkurrenskraftigt näringsliv och ett hållbart samhälle. RISE 2 800 medarbetare driver och stöder alla typer av innovationsprocesser. Vi erbjuder ett 100-tal test- och demonstrationsmiljöer för framtidssäkra produkter, tekniker och tjänster. RISE Research Institutes of Sweden ägs av svenska staten.

RISE Research Institutes of Sweden AB Box 857, 501 15 BORÅS, SWEDEN Telephone: +46 10-516 50 00 E-mail: info@ri.se, Internet: www.ri.se	[Section] RISE Report **: 2023:24** ISBN: **978-91-89757-69-1**